Supporting information for

Towards deep-UV surface-enhanced resonance Raman spectroscopy of explosives: Ultrasensitive, real-time and reproducible detection of TNT

Shankar K. Jha,[†] *Yasin Ekinci,* [*†‡] *Mario Agio,*[§] *Jörg F. Löffler*[†]

[†]Laboratory of Metal Physics and Technology, Department of Materials, ETH Zürich, Switzerland

[‡]Laboratory of Micro- and Nanotechnology, Paul Scherrer Institute, 5232 Villigen-PSI, Switzerland

[§] National Institute of Optics (INO-CNR) and European Laboratory for Nonlinear Spectroscopy (LENS), via Nello Carrara 1, 50019 Sesto Fiorentino (FI), Italy

1. Sample preparation

Al nanoparticle (NP) arrays were fabricated using extreme-UV interference-lithography (EUV-IL) at the XIL-II beamline of Swiss Light Source (SLS), Paul Scherrer Institute (PSI), Switzerland. We started by spin-coating a 100-nm-thick layer of poly(methyl methacrylate) (PMMA) and 30-nm-thick layer of hydrogen silsequioxane (HSQ) on high-purity fused silica (FS) substrates (Suprasil, Heraeus). The top photoresist layer, HSQ, was exposed to multiple-beam interference patterns from 13.5 nm EUV radiation. Subsequent development of HSQ in 25% tetramethylammonium hydroxide (TMAH) solution generated hole-arrays. The hole array in HSQ acted as a mask for further pattern transfer into the PMMA layer by using reactive ion etching with oxygen-plasma (PlasmaLab 80, Oxford Instruments). This was followed by e-beam assisted physical vapor deposition (Univex 500, Oerlikon Leybold Vacuum) of 70-nm-thick Al trough the polymer mask. Finally, the lift-off process in acetone resulted in the Al NP arrays. Scanning electron microscope (SEM) (SU70, Hitachi) images of the substrate were acquired after finishing all the spectroscopic measurements. A thin layer of Cr was deposited before SEM inspection to prevent sample charging.

2,4,6-trinitrotoluene (TNT) as 1 mg/ml solution in acetonitrile (ACN) was purchased from LGC Standards a local distributor of Cerilliant Corporation. This solution was diluted further by the serial dilution process using HPLC grade ACN (Sigma-Aldrich). TNT molecules were deposited onto the substrates by the drop-coating method, where the solution spread over the substrate with a diameter of 5 mm.

2. Optical setup

A home-built optical system was used for absorption, LSPR and Raman measurements. Briefly, a simple combination of a UV focusing objective (NA = 0.4, f = 10 mm; Microspot, Thorlabs) and tube lens (f = 200 mm; Mitutoyo) serves as a functional UV-microscope with an effective magnification of 20×. Grating monochromator (SpectraPro2500i, Princeton Instruments) coupled to a UV optimized, back illuminated, liquid nitrogen cooled CCD detector (Pixis: 2K/BUV, Princeton Instruments) serves as imaging spectrometer. A fiber coupled deuterium-halogen broadband source (Micropak-DH 2000, Ocean Optics) was used for absorption and LSPR measurements. The micro-Raman spectra were acquired in 180° backscattering configuration using 257 nm continuous wave laser excitation from an argon-ion laser (Innova 90 C FreD, Coherent Inc.). A Rayleigh edge filter (Semrock Inc.) – a long pass optical filter – with an optical density > 6 at 257 nm, is used to block the elastically scattered light from entering the spectrometer. The laser spot size at the sample was measured to be ~1 µm. A UV enhanced holographic grating having 2400 lines/mm and blazed at 240 nm was used for Raman measurements. An external shutter was added to block the laser beam and avoid sample photodegradation while not acquiring any signal.

3. Absorption spectra

In Figure S1, the absorption spectra of TNT in solution and solid phases are presented. Solution phase measurements were made in a quartz cuvette having a path length of 1 mm that contained 0.01 mg/ml solution of TNT in ACN. The solid phase measurements were made after drop-coating of 1µL of TNT solution on a fused silica slide. While the absorption maximum for TNT in solution was observed to be ~ 230 nm, it was slightly red-shifted in the solid phase. Since the excitation wavelength used for Raman measurements was 257 nm the absorption red-shift results in better resonance Raman enhancement.

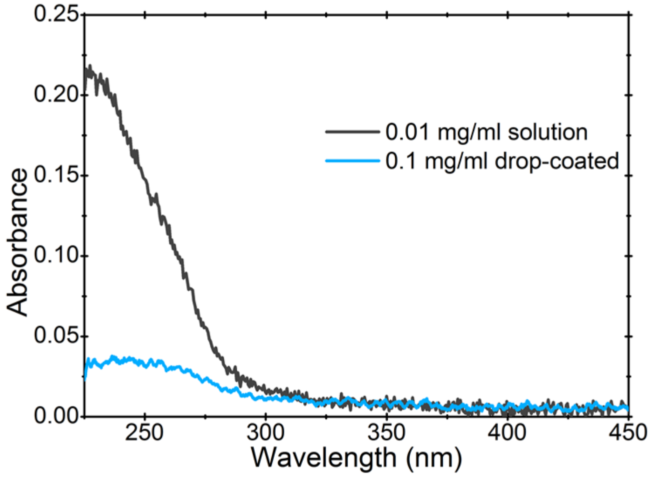

Figure S1: *Absorption spectra of 0.1 mg/ml TNT solution in acetonitrile measured in a quartz cell of 1 mm path length (black line) and 1 µL of 0.1 mg/ml TNT drop-coated on the fused silica slide (blue line). Laser excitation wavelength is indicated. Slight red shift in the absorption maximum is observed from solid sample. This results in better resonance Raman enhancement.*

Figure S1 provides also information about the density of molecules on the surface. The absorbance of solution through 1 mm path length corresponds to 10 femtogram/μm^2 (0.01 mg/ml×1 mm = 10^{-3} mg/cm^2 = 10 femtogram/μm^2). Assuming the absorption cross sections of TNT molecules in liquid and dried molecules on the surface are same, from the ratio of absorption in Figure S1, we obtaion about 1.7 femtogram/μm^2 of TNT on surface and 1.3 femtogram within the laser spot of 1 μm diameter. From the drop-coating of 1 μl of 0.1 mg/ml TNT solution spreading over a 5 mm spot, we estimate the mass of the molecules present in the focus to be 4 femtograms. The difference between the two methods of estimation can be attributed to the molecules that are accumulated on the outer boudaries.

2. Photodegradation of TNT

One of the drawbacks of using DUV excitation for Raman measurements is sample photodegradation. The high-energy photons could cause structural damage to the analyte molecules or might result in its oxidation in the presence of surrounding air. The effect of photodegradation is clearly seen in the Raman spectra, presented in Figure S2 for drop-coated TNT. The signal was collected sequentially from the same location on the sample surface with an exposure time of 1 s for each acquisition. The decrease in Raman intensity is clearly seen. It can also be observed that the Raman band at 1354 cm^{-1} decays much faster than the band at 1624 cm^{-1}. Thus if longer detection times are required, the contribution from the latter band would be higher.

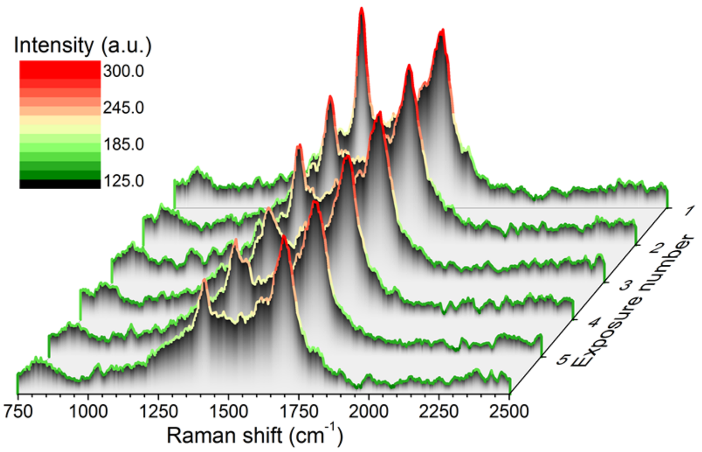

Figure S2: *SERRS spectra of TNT acquired with an exposure time of 1 s and incident optical power of 1 mW. All the spectra were acquired at the same position on the NP array. The effect of photodegradation is clearly seen. It can observed that the peak at 1354 cm*$^{-1}$ *decays much faster than the one at 1624 cm*$^{-1}$

It was observed that the transmission of the sample reduced at the locations where the Raman measurements were done. The optical image of one such area is presented in Figure 1(c) in the manuscript. When Raman measurements were carried out by scanning the sample across the laser beam, a dark trace remained at the scanned location. In Figure S3 the SEM images of one such scanned region is presented.

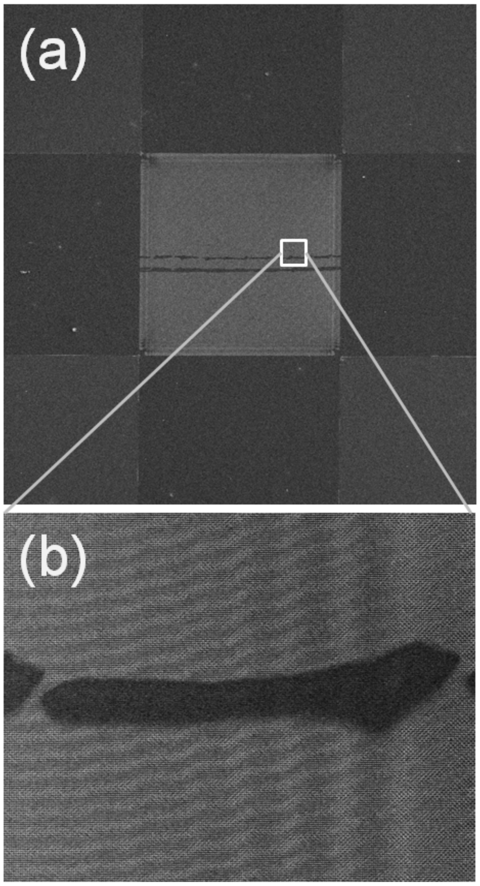

Figure S3: *SEM image of the NP area where Raman measurements were done by continuously moving the sample during signal acquisition. Note: In the boxed area in Figure 1(c) the spots* *where measurements were made are clearly seen. Some photodegradation byproduct is formed during exposure that increases the background in Figure 1(d). By continuously moving the sample stage during signal acquisition the effect of photodegradation is reduced. This results in better SNR.*

3. AFM measurements AFM measurements to determine the formation of TNT crystals and to evaluate the homogeneity of the deposited TNT film on the substrates were made using the Dimensions-3000 AFM probe (Bruker). Measurements were done before and after drop coating 1µL of 0.1 mg/ml TNT on the substrate. In Figure S4 (a) and (b), AFM images of uncoated bare and NP area respectively are presented. In Figure S4 (c)-(f), the AFM images refer to the TNT deposited substrate. The scanned area is 10 µm × 10 µm in (a)-(d), 50 µm × 50 µm in (e), and 25 µm × 25 µm in (f). While it is clear from the panels on the left that micro-crystals are formed on the drop-coated bare areas, this is not obvious from the panels on the right. The brighter patches on the images in Figure (b) and (d) appear to be some defects on the sample as the z-scale has a maximum of 100 nm. No crystallites formation is seen on relatively larger scan area in Figure 3(f). The crystallites present in Figure S4(e) have a height of ~ 500 nm. This can be seen more clearly in Figure S5. The height of individual crystals ranged between 0.3 to 0.5 µm. Thus, it could be concluded that the TNT spreads uniformly on the NP arrays while agglomerations are formed on the bare areas.

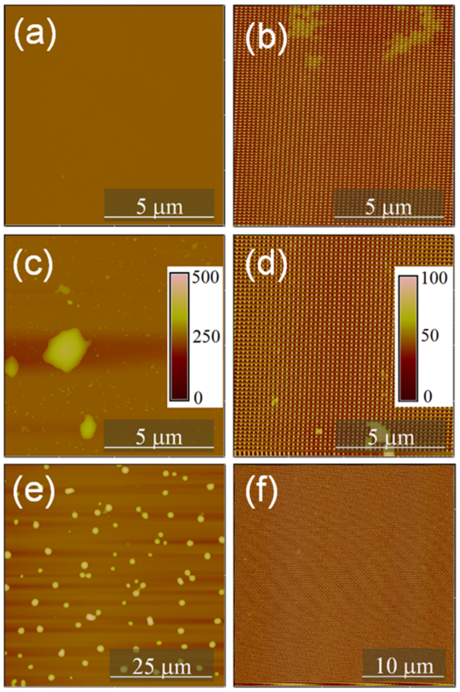

Figure S4: *AFM images of uncoated ((a) and (b)) and TNT coated ((c) – (f)) areas on the substrate. Images on the left side were acquired on the bare areas and the ones on the right side were acquired on the NP array.*

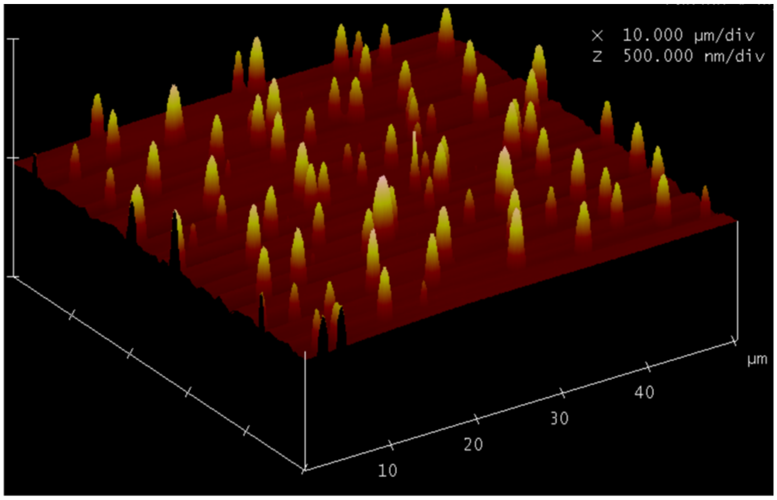

Figure S5*: AFM image of 1 µL of 0.1 mg/ml TNT drop-coated on the bare area of the substrate. Micro crystals have a height of ~ 0.3 – 0.5 µm and can be clearly seen.*

4. FDTD simulations

Simulations based on the finite-difference time-domain (FDTD) method were carried out to explore and gain insight into the far-field and near-field optical properties of the NP arrays. The NPs are modeled as tapered cylinder having an Al core and surrounded by a 3 nm thick oxide shell. The diminution angle (θ) that defined the extent of tapering was assumed to be 12°, a valued extracted from the SEM analysis of individual NPs. A uniform square mesh of 1 nm pitch was used for discretization of the simulation domain. As indicated in Figure S6, the simulation volume is limited to the unit cell of the NP array with the NP at the center of the domain. Appropriate boundary conditions are employed to take into account the periodicity of the nanostructure and its finite extent in the z-direction. The height of the simulation volume is 400 nm. The Drude-Lorentz model with optical constants tabulated in *Handbook of Optical*

Constants of Solids, ed. E. D. Palik and G. Ghosh, (Academic Press, 1998) was used to model the material properties. While a Gaussian pulse is the excitation source for evaluating the extinction spectra, a plane wave (257.2 nm) with electric field parallel to the top surface of the NP is used for modeling the EM near field.

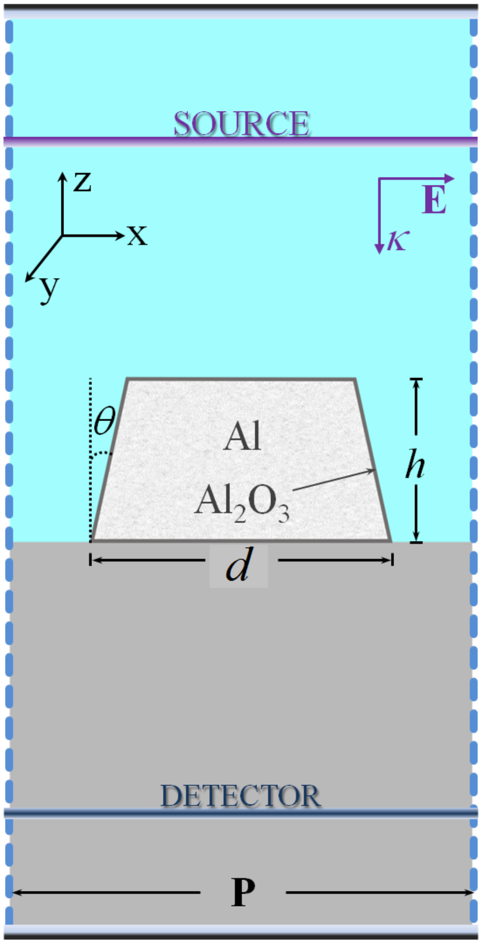

***Figure S5**: Schematic diagram of the simulation domain indicating the various particle parameters diameter (d), height (h), period (P) and diminution angle (θ).*